

Detuning Properties of RF Phase Modulation in the Electron Storage Ring KARA

A. Mochihashi, S. Maier, E. Blomley, M. Schuh, E. Huttel, T. Boltz, B. Kehrer, A.-S. Müller,
Karlsruhe Institute of Technology, Hermann-von-Helmholtz-Platz 1, 76344 Eggenstein-Leopoldshafen, Germany

D. Teytelman

Dimtel, Inc., 2059 Camden Avenue, San Jose, California 95124, USA

(Dated: December 1, 2021)

In electron storage rings, it is possible to increase the electron bunch length by applying a phase modulation on the radio frequency accelerating field by choosing appropriate parameters for the modulation. Such a bunch lengthening effect improves beam parameters such as the beam lifetime, which can help us to get better beam stability. The dependence of the bunch lengthening on the modulation frequency, the so-called detuning property, tends to have a peak with asymmetric slopes around it. The modulation amplitude and the beam current also affect the properties of the detuning condition of such bunch lengthening. We have investigated the detuning property with systematic measurements at the electron storage ring KARA. The experimental results agree with the theoretical model and the simulation results.

I. INTRODUCTION

In high energy electron storage rings dedicated to high energy physics and synchrotron radiation experiments, it is quite essential to prepare stable beams for long-term and precise measurements and experiments. One of the main parameters which show the beam stability is the beam lifetime which corresponds to the loss rate of the particles in the stored beam per unit time. To compensate for the beam loss, an operation scheme, called top-up operation, has been nowadays widely applied to electron storage ring facilities. In this scheme, an additional electron beam is injected repeatedly from the injection accelerator into the storage ring to keep the electron beam current constant. However, the beam lifetime is still significant in such an operation scheme because the lifetime determines the repetition rate of the beam injection, which relates to accelerator operation issues such as radiation protection, energy consumption and operation stability.

There are several processes which can lead to particle loss in the stored electron beam. A beam loss which comes from several scattering processes between the high energy electrons and residual gas molecules happens, and its process depends on the vacuum pressure and the physical aperture conditions of the accelerator. The beam lifetime from these scattering processes is called vacuum lifetime and does not depend directly on the beam current and number of the electrons in one electron bunch.

On the other hand, there is another scattering process in which the number of electrons in the stored beam decreases; the scattering process between the high energy electrons in the same beam bunch. Because the transverse momentum of the electrons which comes from the betatron oscillation can change to the longitudinal momentum due to the scattering process on the transverse plane, the electrons could have more considerable longitudinal momentum which is beyond the momentum acceptance of the storage ring. This beam loss effect which comes from the electron-electron scattering in the same

electron bunch is called Touschek effect, and the beam lifetime from this effect is called Touschek lifetime. The Touschek lifetime depends mainly on the electron density in one electron bunch and the momentum acceptance of the accelerator. There is another beam loss process which comes from quantum excitation due to the emission of photons from the high energy electrons. The beam lifetime from this quantum effect is called the quantum lifetime and can take on very high value compared to the vacuum and Touschek lifetime under normal conditions of the accelerator operation.

In principle, it is possible to improve the beam lifetime in the electron storage ring by manipulating the operating condition of the accelerator. One of the promising ideas is to elongate the longitudinal bunch distribution to relax the Touschek effect by decreasing the electron density in the electron bunch. In electron storage rings, additional radio frequency (rf) cavities, whose operating frequency is an integer harmonic of the rf cavities which are used to accelerate the beam, can manipulate the electron bunch length. The method by using such an additional cavity, called harmonic cavity or Landau cavity, has been firstly proposed and investigated for the proton synchrotrons[1–3], and has been later operated at an electron storage ring[4]. These harmonic cavities were initially used to suppress collective beam instabilities such as the coupled bunch instability due to the Landau damping process. The harmonic cavity, however, can increase not only the frequency spread of the synchrotron oscillation but also the longitudinal bunch length because of the deformation of the longitudinal potential well structure. This bunch lengthening scheme has now been considered and applied to several electron storage rings, especially for the synchrotron radiation light sources with small beam emittance [5–10].

Ideally, the storage ring contains such an additional cavity system. However, it is challenging to install such system into compact electron storage rings with shorter circumferences because the number and length of the straight sections in the ring could be one of the un-

avoidable restrictions for installing such additional beam instrumentation. An alternative idea for the harmonic cavity system is to manipulate the electron distribution on the longitudinal phase space by modulating the phase of the rf accelerating field with proper modulation frequencies. This rf phase modulation scheme is applicable if the rf system can operate the phase modulation; advantageously, this scheme is available without installing beam instrumentation into the storage ring.

In the Photon Factory electron storage ring in High Energy Accelerator Research Organization (KEK), they experimented with the bunch lengthening by the rf phase modulation whose modulation frequency was twice the synchrotron oscillation frequency and confirmed not only the improvement of the beam lifetime but also stabilisation of the longitudinal-coupled-bunch instability[11, 12]. In this previous study, they have also discussed the beam dynamics under the phase modulation with a theoretical model and simulations based on macro-particle tracking. The experimental results and the simulations have shown that the longitudinal distribution of the electrons tends to have the quadrupole oscillation mode accompanied by the bunch lengthening. In the Brazilian synchrotron light source, they experimented with suppressing the longitudinal coupled bunch instability by the rf phase modulation[13]. In this previous study, they have discussed the beam dynamics based on the Hamiltonian formalism and existence of 2 or 3 stable fixed points on the longitudinal phase space from the rf phase modulation. They have also discussed the number of the fixed points and the area of the stable region on the longitudinal phase space, and have shown the change in the rf bucket structure for the phase modulation frequency, which implies a detuning property of the bunch lengthening for the modulation frequency. In the electron storage ring DELTA operated by the TU Dortmund University, they investigated the damping process of coupled bunch instabilities by the rf phase modulation and a digital bunch-by-bunch feedback system[14]. From the experimental results and the numerical simulation based on the macro-particle tracking, they have discussed the dependence of the damping time on the phase modulation amplitude. By switching the beam excitation on and off by the bunch-by-bunch feedback system and constructing a relevant model to analyze the damping time due to the rf phase modulation, they have shown a quadratic dependence of the damping time on the phase modulation amplitude[15, 16].

At the KIT synchrotron where 2.5 GeV electron storage ring KARA (Karlsruhe Research Accelerator)[17] is in operation, we have introduced the function of the rf phase modulation into the low-level rf (LLRF) system of KARA by which we can change both the frequency and amplitude of the rf phase modulation quite easily. Because the maximum beam energy from the injection accelerator in KARA is 500 MeV, after the injection into the storage ring, we ramp the beam energy up to 2.5 GeV with the storage ring in regular accelerator operation.

Therefore, it is essential for KARA to improve the beam lifetime, so that the experiments with the synchrotron radiation from KARA take place with enough beam stability. To introduce the rf phase modulation scheme into KARA accelerator operation, we have searched for the optimum condition to improve the beam lifetime by focusing mainly on three parameters and conditions for the rf phase modulation, namely, the frequency and the amplitude of the modulation, and the beam current. Because KARA does not have the possibility of the top-up operation in 2.5 GeV, it seems essential to investigate the range of the optimal parameters in dependency of the beam current. In the process to find the optimum condition of the rf phase modulation, we have discussed the detuning properties of the bunch lengthening when we slightly change the modulation frequency around twice the synchrotron frequency. We discuss a theoretical model which shows us that the dependence of the bunch length on the modulation frequency could have an asymmetric peak around the frequency of twice the synchrotron frequency, and the experiments of the bunch length measurement with the streak camera and the rf phase modulation agree with the model. The results of the simulation based on macro particle tracking follow these results.

In section II, we discuss the theoretical model which describes the beam dynamics with the rf phase modulation and the detuning properties of the bunch lengthening. In section III, we discuss the simulation results for the longitudinal beam dynamics based on the macro-particle tracking method with the effect of the rf phase modulation. In section IV, we discuss the bunch length measurement with the streak camera and rf phase modulation under several different conditions. Finally, we summarise our discussion and future plans in section V.

II. THEORETICAL MODEL

In the reference[11], they have discussed the motion of the electron under the influence of the rf phase modulation whose modulation frequency is twice the synchrotron oscillation frequency. In this section, we also discuss the motion of the electron in the same manner as [11] but by adding a detuning condition into the modulation frequency; namely, we formulate the equation of motion in the case that the modulation frequency is slightly different from twice the synchrotron oscillation frequency.

The equation of motions of the electron for the longitudinal direction can be written as[11]

$$\frac{d\tau}{dt} = -\alpha\delta, \quad (1)$$

$$\frac{d\delta}{dt} = \frac{eV_c \cos(\phi_0 - \omega\tau + \phi_m) - U_0}{T_0 E_0} - 2\gamma_e \delta. \quad (2)$$

Here τ and δ correspond to the time and relative energy difference between the electron and the synchronous conditions, α is the momentum compaction factor, V_c is the

amplitude of the rf acceleration voltage, ϕ_0 is the synchronous phase of the electron beam, ω is the angular frequency of the rf accelerating field, U_0 is the energy loss of the electron due to the synchrotron radiation, T_0 is the revolution period of the electron, and E_0 is the electron beam energy. The second term of the right-hand side in Eq. (2) corresponds to the radiation damping term with the factor γ_ϵ ,

$$\gamma_\epsilon = \frac{1}{2T_0} \left(\frac{dU}{dE} \right)_{E_0}. \quad (3)$$

Here U is the synchrotron radiation loss, and E is the beam energy. The phase ϕ_m represents the phase modulation factor, and now we assume ϕ_m has the following modulation characteristics.

$$\phi_m = \phi_{m0} \cos((2\omega_s + \Delta\omega)t), \quad (4)$$

where ϕ_{m0} is the modulation amplitude, ω_s is the angular frequency of the synchrotron oscillation, and $\Delta\omega$ corresponds to the detuning frequency of the phase modulation from $2\omega_s$. By applying the linear approximation which comes from the small amplitude of the synchrotron oscillation and the phase modulation, we get the equation of motion for the electron which performs the synchrotron oscillation with the phase modulation[11]:

$$\frac{d^2\tau}{dt^2} + 2\gamma_\epsilon \frac{d\tau}{dt} + \omega_s^2 (1 + \epsilon \cos(2\omega_s + \Delta\omega)t) \tau = 0, \quad (5)$$

where $\epsilon = \phi_{m0} \cot \phi_0$. To solve Eq. (5) we assume the following solution for τ :

$$\tau = a(t) \sin \omega_s t + b(t) \cos \omega_s t, \quad (6)$$

with the following restriction[18]:

$$\dot{a}(t) \sin \omega_s t + \dot{b}(t) \cos \omega_s t = 0. \quad (7)$$

Now we consider only the change in τ with slow time variation compared to the synchrotron oscillation period and perform the averaging with time for Eq. (5). From the averaging we get the equations for the amplitude function $a(t)$ and $b(t)$ in Eq. (6):

$$\begin{pmatrix} \dot{a}(t) \\ \dot{b}(t) \end{pmatrix} = -\gamma_\epsilon \begin{pmatrix} 1 & 0 \\ 0 & 1 \end{pmatrix} \begin{pmatrix} a(t) \\ b(t) \end{pmatrix} + \frac{\omega_s \epsilon}{4} \begin{pmatrix} \sin \Delta\omega t & -\cos \Delta\omega t \\ -\cos \Delta\omega t & -\sin \Delta\omega t \end{pmatrix} \begin{pmatrix} a(t) \\ b(t) \end{pmatrix} \quad (8)$$

If we assume the complex function $\xi(t) = a(t) + ib(t)$, Eq. (8) can be written as a simple form:

$$\dot{\xi}(t) = -\gamma_\epsilon \xi(t) + \frac{\omega_s \epsilon}{4} e^{i(\Delta\omega t - \frac{\pi}{2})} \xi(t). \quad (9)$$

Eq. (9) can be solved analytically and the solution is given by

$$\xi(t) = \xi_0 \exp\left(-\gamma_\epsilon t + \frac{\omega_s \epsilon}{4} (\cos \Delta\omega t + i \sin \Delta\omega t)\right), \quad (10)$$

where ξ_0 is a constant. Therefore, the solutions for $a(t)$ and $b(t)$ are given as

$$\begin{aligned} a(t) &= \xi_0 \exp\left(-\gamma_\epsilon t + \frac{\omega_s \epsilon}{4} \cos \Delta\omega t\right) \\ &\quad \times \cos\left(\frac{\omega_s \epsilon}{4} \sin \Delta\omega t\right), \end{aligned} \quad (11)$$

$$\begin{aligned} b(t) &= \xi_0 \exp\left(-\gamma_\epsilon t + \frac{\omega_s \epsilon}{4} \cos \Delta\omega t\right) \\ &\quad \times \sin\left(\frac{\omega_s \epsilon}{4} \sin \Delta\omega t\right). \end{aligned} \quad (12)$$

Equations (11) and (12) show that the amplitude of the electron can change with time due to the oscillation term in the growth and damping part. If we consider the condition in which these amplitude functions have the local minimum or maximum values, namely, $\dot{a}(t) = \dot{b}(t) = 0$, the time t_0 at the local minimum or maximum values can be written as

$$t_0 = \frac{1}{\Delta\omega} \left(2\pi n - \sin^{-1} \left(\frac{4\gamma_\epsilon}{\omega_s \epsilon} \right) \right), \quad (13)$$

where n is an integer. If the detuning frequency $\Delta\omega$ is small compared to the synchrotron oscillation frequency, the periodic change in the amplitude is much slower than the synchrotron oscillation. Therefore, the root mean square value of the amplitude of the electron τ with the time averaging $\sqrt{\langle \tau^2 \rangle}$ is given as

$$\sqrt{\langle \tau^2 \rangle} = \frac{\xi_0}{\sqrt{2}} \exp\left(-\frac{2\pi n \gamma_\epsilon}{\Delta\omega} + \frac{\omega_s \epsilon}{4} \cos\left(\sin^{-1}\left(\frac{4\gamma_\epsilon}{\omega_s \epsilon}\right)\right)\right), \quad (14)$$

where we assume $2\pi n \gg \sin^{-1}\left(\frac{4\gamma_\epsilon}{\omega_s \epsilon}\right)$. As seen in Eq. (14), the time-averaged amplitude of the electron depends on the detuning frequency $\Delta\omega$ and its dependency is mainly given as $\exp\left(-\frac{2\pi n \gamma_\epsilon}{\Delta\omega}\right)$. This implies that the amplitude with non-zero detuning frequency depends on the signature of the detuning $\Delta\omega$. If we measure the dependence of the bunch length on the detuning frequency, the detuning property could have a peak at $\Delta\omega = 0$ with asymmetric slopes for negative and positive detuning conditions around the peak.

Eq. (14) shows the amplitude of the electron decreases exponentially with the radiation damping and the constant excitation term from the phase modulation. Because of the radiation excitation which we do not include into Eq. (5), the amplitude can keep non-zero value but different from the amplitude without the phase modulation. The theoretical model in Eq. (5) applies the linear approximation in which we assume the amplitude of the electron is small, and the first-order approximation is valid. However, it is possible to increase the parameter ϵ until the linear approximation is not valid any more. In this case, the structure of the longitudinal potential called rf bucket could change from normal parabolic to distorted form under the condition of the overexcitation, and the bunch structure could change accordingly.

III. SIMULATION

To investigate the beam dynamics under the phase modulation with frequency detuning, we have performed numerical simulations based on macro-particle tracking. The used method is based on[11]. We have calculated the equations of motion for the longitudinal direction stated in Eqs. (1) and (2) numerically while considering the transient beam loading effect which comes from the beam-induced voltage in each rf accelerating cavity in KARA storage ring. In the simulation, we have treated the rf accelerating voltage $V_c = |\vec{V}_c|$ as the vector sum of the generator voltage \vec{V}_g and the beam-induced voltage \vec{V}_b , namely, $\vec{V}_c = \vec{V}_g + \vec{V}_b$. \vec{V}_g has the effect of the phase modulation directly, and both of \vec{V}_c and \vec{V}_b have been changed due to the phase modulation accordingly. To consider the transient beam loading effect, we have treated both the phase advance and the amplitude of the beam-induced voltage \vec{V}_b between adjacent bunches in multi-bunch filling condition with the same method as in[11]. Because of the characteristics of the transient beam loading effect, initially \vec{V}_b inside each cavity can change with the beam revolution step. Therefore, we have performed in the simulation enough revolution steps to get quasi-stable condition in which \vec{V}_b and \vec{V}_c can oscillate slightly but do not change drastically. Typically we have performed the revolution step with the period longer than $\frac{2}{\gamma_e}$. To get the realistic solution for the motion of the electron, we have introduced the radiation excitation into Eqs. (1) and (2) as a random walk of the energy spread which has Gaussian distribution with its standard deviation σ_r as

$$\sigma_r^2 = 4\gamma_e T_0 \left(\frac{\sigma_\epsilon}{E_0} \right)^2, \quad (15)$$

where σ_ϵ is the natural energy spread.

We have prepared 10000 macro-particles for each bunch and calculated the distribution of the electrons on the longitudinal phase space for each bunch for Karlsruhe Research Accelerator (KARA) storage ring with 2.5 GeV operation. The main parameters of the KARA storage ring are summarised in Table I. To calculate the generator voltage \vec{V}_g and the beam-induced voltage \vec{V}_b we have used the measured values of the shunt impedance, the unloaded quality factor, and the input coupling value for each cavity, which were measured at the installation of them into the KARA storage ring.

In the simulation, we have considered three tuning parameters of the rf phase modulation: the modulation frequency, the modulation amplitude, and the beam current. In the following, we discuss the dependence of the bunch lengthening on these parameters.

A. Modulation frequency

Fig. 1 and 2 show the simulation results of the particle distribution on the longitudinal phase space. Fig. 1 is the result without the phase modulation. On the other hand, Fig. 2 is the result with the phase modulation whose modulation frequency is equal to $2f_s$ and modulation amplitude of 100 mrad. In these simulations, we have assumed a multi-bunch filling pattern of KARA storage ring which has three bunch trains with empty rf buckets between them and the total beam current of 150 mA. On these figures, we can see the phase space distribution changes clearly due to the phase modulation. On Fig. 2 we have plotted two snapshots of the phase space distribution when the phase modulation is active. These results show that both, the bunch length and the energy spread, change under the phase modulation, and the modulation looks like the quadrupole oscillation mode on the longitudinal direction. Fig. 3 is a colour map to show the change in the longitudinal electron distribution in one bunch for a typical time scale of the synchrotron oscillation period when we set the modulation frequency as $2f_s$. In this case, f_s is equal to 30.89 kHz, which corresponds to the period of 32.37 μ s. We can see the bunch length changes periodically with a period of around half of the synchrotron oscillation period. Fig. 3(b) and 3(c) show the color maps when we shift the modulation frequency from $2f_s$ with negative (-1 kHz) and positive (+1 kHz) detuning, respectively. As shown in the figure, negative detuning condition can effectively lead to a bunch lengthening compared to the resonance condition and the positive detuning. By scanning the modulation frequency, we have summarised the dependence of the bunch lengthening on the detuning frequency. Fig. 4 and 5 show snapshots of the longitudinal phase space for both detuning conditions in Fig. 3(b) and 3(c). From these figures, we can see that the longitudinal particle distribution changes significantly under the negative detuning in particular. Two spiral arms appear from the central core of the particle distribution, which

TABLE I. Main parameters of KARA storage ring.

Parameter	Symbol	Value	Unit
Beam energy	E_0	2.5	GeV
rf frequency	f_{rf}	499.731	MHz
Harmonic number	h	184	
Total accelerating voltage	V_c	1.4	MV
Radiation loss per turn	U_0	622.4	keV
Momentum compaction factor	α	0.00867	
Natural energy spread	$\frac{\sigma_\epsilon}{E_0}$	9.08×10^{-4}	
Natural bunch length	σ_t	36.9	ps
Beam current (typ.)	I_b	150	mA
Number of rf sections		2	
Number of cavities per 1 rf section		2	

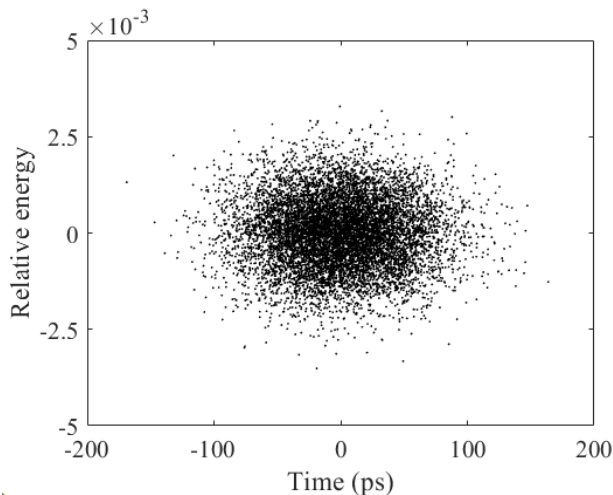


FIG. 1. The simulation result of the longitudinal phase space distribution when the rf phase modulation is not active. We assume the total beam current of 150 mA in a multi-bunch condition in KARA storage ring.

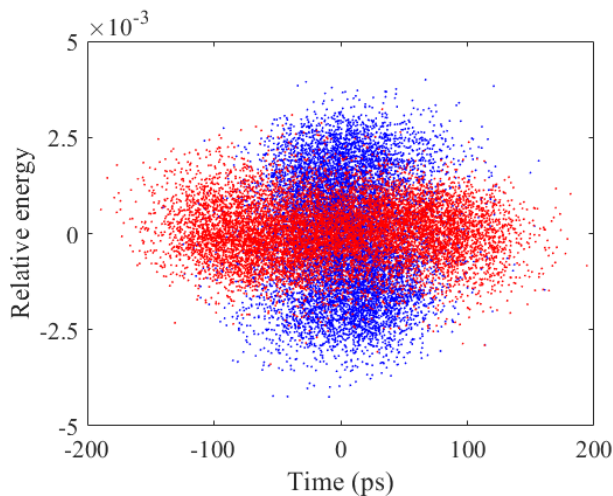


FIG. 2. The simulation result of the longitudinal phase space distribution when the rf phase modulation is active. The modulation frequency is equal to $2f_s$, and the amplitude is 100 mrad. The blue and red dots correspond to the snapshots of the electron distribution at different phases of synchrotron motion.

could cause the sub-bunches inside one rf bucket. Fig. 6 shows a dependence of the bunch length on the detuning frequency from $2f_s$. To analyse the bunch length on Fig. 6 we have evaluated the averaged bunch length along the horizontal axis on Fig. 3(a)-(c). This 'detuning' curve has its peak at the negative detuning side and the asymmetric slopes for both negative and positive sides. The difference in the gradient between the negative and positive sides agrees with the theoretical model in Eq. (14) in which the negative slope ($\Delta\omega < 0$) should have a gradual slope.

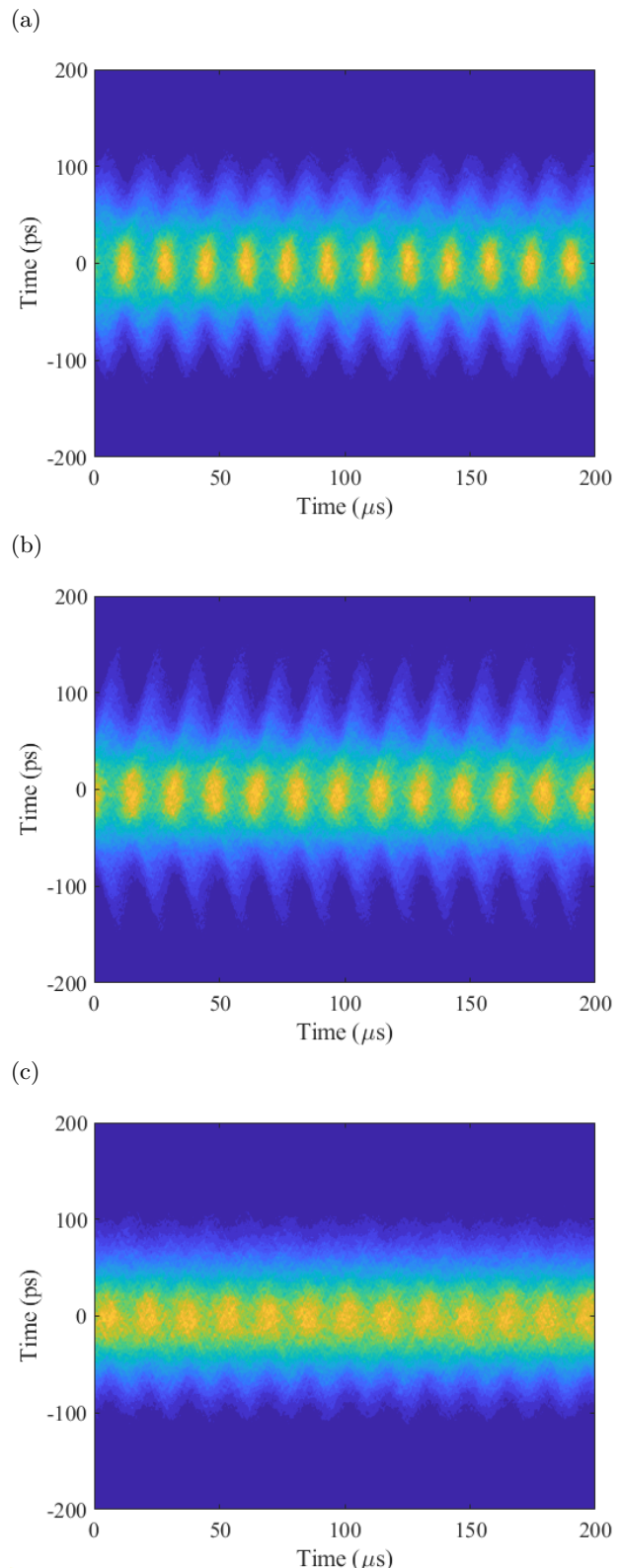


FIG. 3. The simulation result of the change in the longitudinal electron distribution in one bunch when the modulation frequency is $2f_s$ (upper, Fig. 3(a)), $2f_s-1$ kHz (middle, Fig. 3(b)), and $2f_s+1$ kHz (lower, Fig. 3(c)). The horizontal scale (200 μs in full scale) corresponds to 12.4 times half of the synchrotron oscillation period. The condition of the machine parameters is the same as in Fig. 2. The vertical scale shows the measure of the bunch length. The positive direction on the vertical axis correspond to the head of the bunch. The blue and yellow colour indicate low and high electron density in the charge distribution, respectively.

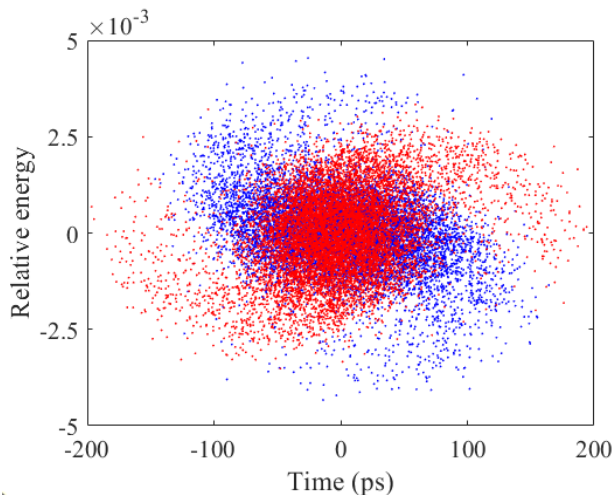


FIG. 4. The simulation result of the longitudinal phase space distribution when the rf phase modulation is active. The blue and red dots correspond to the snapshots of the electron distribution at different phases of synchrotron motion. The conditions and setting are the same as Fig. 3(b) (1 kHz negative detuning).

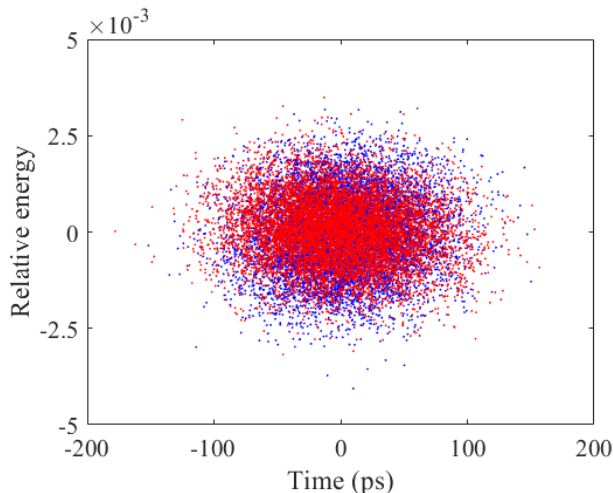


FIG. 5. The simulation result of the longitudinal phase space distribution when the rf phase modulation is active. The blue and red dots correspond to the snapshots of the electron distribution at different phases of synchrotron motion. The conditions and setting are the same as Fig. 3(c) (1 kHz positive detuning).

B. Modulation amplitude

The bunch lengthening due to the phase modulation depends not only on the modulation frequency but also on the modulation amplitude. Fig. 7 shows three detuning curves for different modulation amplitudes: 50, 100 and 200 mrad. As shown in the figure, a larger modulation amplitude enhances the bunch lengthening, and larger amplitude also leads the peak frequency to the negative detuning direction. Fig. 8 shows the time-averaged

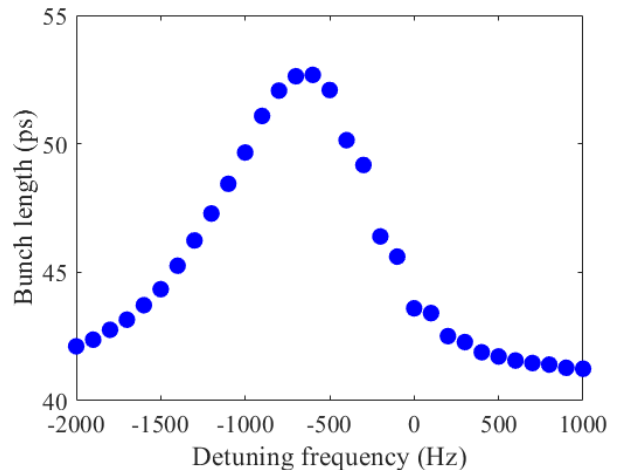


FIG. 6. The simulation result of the detuning curve for the bunch lengthening under the phase modulation. The horizontal axis corresponds to the frequency difference between $2f_s$ and the modulation frequency.

longitudinal bunch structure for each modulation amplitude in Fig. 7 and the natural longitudinal structure. As shown in the figure, the longitudinal distribution becomes non-Gaussian for large modulation amplitudes. At 200 mrad, a new shoulder appears on both sides of the slopes around the peak.

This negative detuning property comes from non-linearity of a harmonic oscillator with larger oscillation amplitude[12], in which the eigenfrequency tends to decrease in larger oscillation amplitude. To discuss the negative detuning at more significant modulation amplitude condition, we have analysed the frequency of each macroparticle by FFT method. Fig. 9(a) shows the spectra for the modulation amplitude of 50 and 200 mrad with the peak frequency of the 50 mrad detuning curve and Fig. 9(b) is the same spectra with the peak frequency of the 200 mrad detuning curve. As seen in these figures, the left and right side peaks on the figures correspond to f_s and $2f_s$ components, and larger amplitude condition tends to have negative frequency shift for f_s peak. This frequency shift can cause the enhancement of the negative detuning on the detuning curves in Fig. 7.

C. Beam current

In the simulation, we have considered the beam loading effect which occurs inside the rf cavities. Therefore the dependence of the bunch lengthening on the beam current could happen. Fig. 10 shows the detuning curves for three different beam current conditions with the same modulation amplitude of 50 mrad. As shown in the figure, the bunch lengthening increases at the high beam current condition by the phase modulation. According to Eq. (5) the driving term from the phase modula-

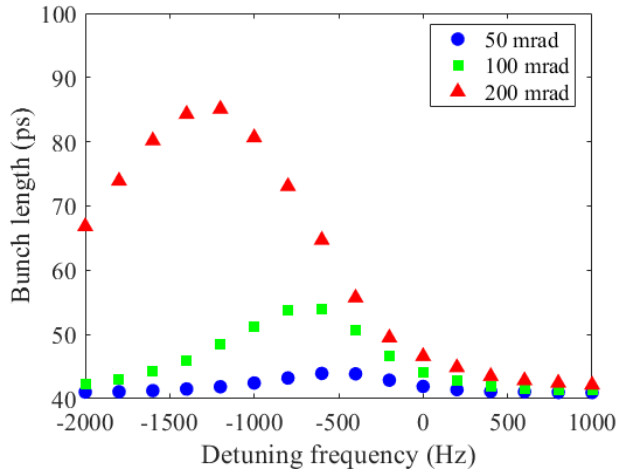


FIG. 7. The simulation result of the detuning curves for the modulation amplitude of 50 mrad (blue circles), 100 mrad (green squares), and 200 mrad (red triangles) at the total beam current of 150 mA.

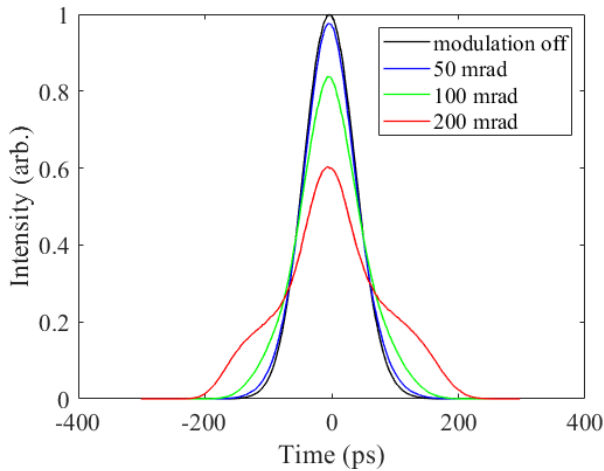


FIG. 8. The simulation result of the longitudinal distribution of the macro-particles in one bunch for the modulation amplitude of 50 mrad (blue), 100 mrad (green), 200 mrad (red), and the modulation off (black).

tion is proportional to the parameter ϵ , which includes $\cot \phi_0$. When the transient beam loading happens inside the rf cavities, the synchronous phase ϕ_0 can change transiently, and that change causes the parameter ϵ . Because the accelerating voltage decreases due to the beam loading, ϕ_0 tends to decrease, and ϵ can increase effectively. Because this effect comes from transient beam loading, it depends on the machine parameters and the filling pattern. In case of the simulation based on a realistic operating condition of KARA storage ring, this dependency is minimal.

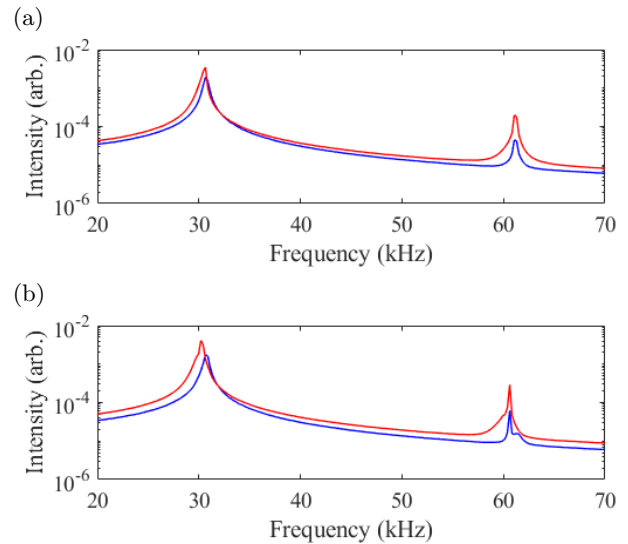


FIG. 9. The averaged frequency spectrum of the motion of each macro particle under different condition of the rf phase modulation. Blue and red curves correspond to the spectrum at the modulation amplitude of 50 and 200 mrad. Upper figure (Fig. 9(a)) is the spectrum at the modulation frequency of $2f_s - 600$ Hz, which is the peak frequency of the 50 mrad detuning curve. Lower figure (Fig. 9(b)) is the spectrum at the modulation frequency of $2f_s - 1200$ Hz which is the peak frequency of the 200 mrad detuning curve.

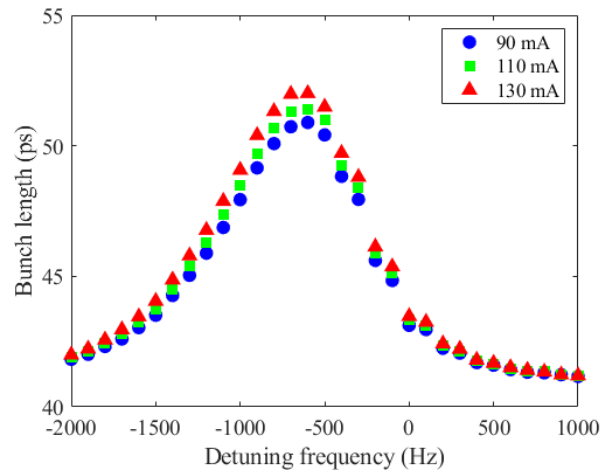


FIG. 10. The simulation results of the detuning curve for different 3 total beam current conditions with the same modulation amplitude of 100 mrad. Blue circles, green squares and red triangles correspond to 90, 110, and 130 mA condition, respectively.

IV. EXPERIMENT

The experiment was carried out at Karlsruhe Research Accelerator (KARA) electron storage ring. Table I summarises the main machine parameters of KARA. In the experiment, we have operated the KARA storage ring

with the same bunch filling pattern as the regular users' operation discussed in section III.

To carry out the rf phase modulation at KARA, we have introduced the modulation function into our low-level RF (LLRF) system (Dimtel, LLRF9/500)[19]. In KARA storage ring, each RF station has one klystron whose maximum output power is 250 kW. Because one RF station has 2 RF accelerating cavities, one klystron drives 2 RF cavities in KARA. To control 2 RF stations independently, each RF station has its LLRF system. From one master oscillator, whose signal frequency is around 500 MHz, each LLRF system in each RF station receives the master clock signal and drives the RF station. Because the LLRF system has the function of the phase modulation, we can perform the phase modulation for each RF station independently. In the experiments discussed in the following part, we performed the phase modulation at only one RF station, which is the same condition as in the simulation. To perform the phase modulation, we set the modulation frequency and the amplitude to the LLRF system remotely. The technical details for the method of the phase modulation by the LLRF system are discussed in[20].

To observe the longitudinal motion of the beam, we use a visible light streak camera (VSC, Hamamatsu, C5680-21S) at the beam diagnostic beam line[21] in KARA. In the beam diagnostic beamline, we can use the synchrotron radiation (SR), which comes from one of the bending magnets in KARA. In the front-end part of the beamline, we use one mirror chamber to filter out the high energy component of the SR beam and to extract the beam from the ultra-low vacuum environment to the atmosphere. Therefore, we can use the visible light component of the SR beam at the beam diagnostic beamline in the atmospheric environment. The streak camera measurement needs to get excellent temporal resolution whose typical time scale is several to ten pico-seconds. To do so, we use a focusing mirror system to avoid the aberration and deliver the spot image into the input slit of the VSC. The VSC has two sweeping units; fast sweeping unit (synchro scan unit) and slow sweeping unit (blanking amplifier unit). By the fast sweeping unit, the VSC can observe the pulse length of the SR beam which corresponds to the electron bunch length in the storage ring with the synchronisation between the sweep timing of the VSC and the revolution timing of the electron beam. By the slow sweeping unit, the VSC can also observe the longitudinal beam motion whose time scale is longer than the revolution period typically. Because these two sweeping units function simultaneously, we can observe both the bunch length and the global longitudinal motion of the beam precisely.

A. Modulation frequency

We have measured the bunch lengthening while changing the modulation frequency. Fig. 11(a), 12(a) and

13(a) show the streak camera images measured with a settled modulation amplitude of 3 degrees (52.4 mrad) and a beam current of 133 mA. Fig. 11(a) shows the streak camera image at the maximum bunch lengthening condition of the modulation frequency. Fig. 12(a) and 13(a) show the image with -1 kHz and +1 kHz detuning from the modulation frequency at Fig. 11(a). As seen in these figures, the electron bunch length oscillates with time and the oscillation frequency is almost the same as twice the synchrotron oscillation frequency. By changing the modulation frequency systematically, we have analysed the detuning curve of the bunch length experimentally, which is similar to Fig. 6. Because the bunch length oscillates with time, we have analysed the streak camera image by averaging along the slow sweeping axis (horizontal axis in Figs. 11(a)-13(a)). Fig. 14 shows the detuning curve of the bunch length from the systematic measurement. To improve the statistics, we have taken 100 image data at each modulation frequency condition—all of the data points in Fig. 14 show the statistical errors; however, the error values are smaller than the marks in this figure. As seen in the figure, the detuning curve has asymmetric slopes around the peak. This tendency agrees with the simulation result (Fig. 6) and the theoretical result qualitatively. Figs.11(b) - 13(b) show the simulation results for the same frequency conditions with the modulation amplitude of 100 mrad (5.7 degrees); Fig. 11(b) is the result at the maximum bunch lengthening condition and Fig.12(b) and 13(b) are the condition with -1 kHz and +1 kHz detuning from the peak frequency. As seen in these figures, the modulation patterns between the streak camera data and the simulation results agree with each other qualitatively despite the difference of the modulation amplitudes between them, namely, in the experiment we could excite the beam with smaller modulation amplitude than that in the simulation. One possible reason for this difference comes from the condition of the beam loading effect in the rf accelerating cavities. In the simulation, we used the cavity parameters measured before the installation into the KARA storage ring. Therefore, the condition of the beam loading effect in the experiment could be different from that in the simulation; small quality factor could cause prominent transient beam loading effect and enhance the phase modulation because of the change in the synchronous phase, as discussed in Sec. III C. The other reason would come from the systematic error of the modulation amplitude. Additional measurements of the cavity parameters and calibration of the modulation amplitude are necessary for future steps. Compared to the detuning curve from the simulation (Fig. 6) and the experiment, the bunch length in the experiment tends to be longer than the simulation at the modulation frequency far from the peak frequency. In the simulation, we do not include other effects which can cause the bunch lengthening such as the potential-well distortion[22]. The difference between them would come from such collective effects.

In the experiment, we have measured the synchrotron oscillation frequency f_s in parallel with the bunch length measurement by using the readout of the beam signal of the bunch-by-bunch feedback system[23]. The measured value of f_s distributed at the centre frequency of 32 kHz with the readout fluctuation of ± 1 kHz. This broad uncertainty comes from the non-negligible width of f_s peak on the frequency spectrum. Because of this uncertainty, it is difficult to discuss the tendency of the negative detuning from the experiments.

B. Modulation amplitude and beam current

We have also measured the bunch length and the detuning curves while changing the modulation amplitude. Fig. 15 shows three detuning curves with the modulation amplitude of 3 degrees (52.4 mrad), 4 degrees (69.8 mrad), and 5 degrees (87.3 mrad). The measurement took place with a beam current of 90 mA. As seen in the figure, the bunch lengthening increases with the modulation amplitude and the peak frequency tends to shift with the negative direction. This tendency agrees with the simulation results shown in Fig. 7 and this negative detuning comes from the characteristics of the non-linear harmonic oscillator system discussed in Sec.III B. Fig. 16(a),(b) shows longitudinal bunch profiles for the modulation amplitudes of 3 and 5 degrees at the peak frequencies for each detuning condition. As seen in the figures, an additional structure appears on both sides of the peak, and the deformation of the peak structure becomes prominent at larger modulation amplitude; in Fig. 16(b) the sub-peaks appear on both sides of the central peak, which implies the formation of the sub-bunches.

To observe the beam loading effect on the bunch lengthening with the phase modulation, we have observed the bunch length and the detuning curves while changing the beam current. By decreasing the accelerating voltage considerably, we can easily change the beam current without any disturbance. After the changing, we have recovered the accelerating voltage again and continued the measurement. Fig. 17 shows three detuning curves with different beam current by keeping the modulation amplitude at the same value (3 degrees). As shown in the figure, the bunch lengthening due to the phase modulation tends to be effective under the higher beam current condition, which corresponds to the simulation results in Fig. 10 qualitatively. This enhancement comes from the transient beam loading effect inside the cavity. Because of the beam loading, the effect of the phase modulation can be effective, and the bunch lengthening becomes prominent. The bunch lengthening in the experiment becomes prominent compared to the simulation results in Fig. 10. This enhancement could come from the difference of the beam loading effect between the experiment and the simulation, as discussed in Sec. IV A.

V. SUMMARY

In high energy electron storage rings dedicated to high energy physics and synchrotron radiation experiments, it is quite essential to prepare stable beams for the experiments. One idea to stabilise the beam and to improve the beam quality is to improve the beam lifetime by lengthening the electron bunch. In this paper, we have discussed the beam dynamics of the rf phase modulation by which the bunch length can change considerably. One of the critical parameters to lengthen the bunch efficiently is the modulation frequency. The modulation frequency should be near to twice the synchrotron oscillation frequency $2f_s$ to excite the quadrupole mode oscillation on the longitudinal phase space. To discuss the detuning property of the bunch lengthening, we have considered a theoretical model which can treat the frequency difference between the modulation frequency and $2f_s$. The theoretical model showed a solution for the dependence of the bunch lengthening on the modulation frequency. This detuning property, called a detuning curve, showed a single peak curve with asymmetric slopes for the positive and the negative frequency sides; namely, the slope of the positive side tends to be steeper than that of the negative side.

To consider the beam dynamics of the phase modulation in-depth, we have performed the simulation based on the macro-particle tracking method. By considering the equations of motion for the longitudinal motion of the electrons with the effect of the rf phase modulation and the transient beam loading effect inside the rf accelerating cavities, we have calculated the behaviour of the electron distribution of the longitudinal phase space. From the results, we have delivered the detuning property of the bunch lengthening, which showed that the detuning curve has the asymmetric aspect around the central peak, which agrees with the theoretical result. Besides, we have considered the effect of the modulation amplitude and the beam current on the detuning property of the bunch lengthening. The results showed that the overexcitation could cause negative detuning for the detuning property of the bunch lengthening due to the non-linear property of the longitudinal motion of the electron, and the phase modulation can function at the higher beam current condition due to the transient beam loading effect.

To consider these results and discussions experimentally, we have introduced the function of the phase modulation into our low-level rf system and experimented at KARA storage ring with 2.5 GeV electron beam. Behaviours of the longitudinal motion of the beam such as the oscillation of the bunch length, which has been measured by the visible light streak camera, agreed with the simulation results qualitatively. However, a quantitative disagreement between the simulation and the experiment about the bunch lengthening remains. This disagreement could mainly come from the difference of the condition of the beam loading effect between the experiment and

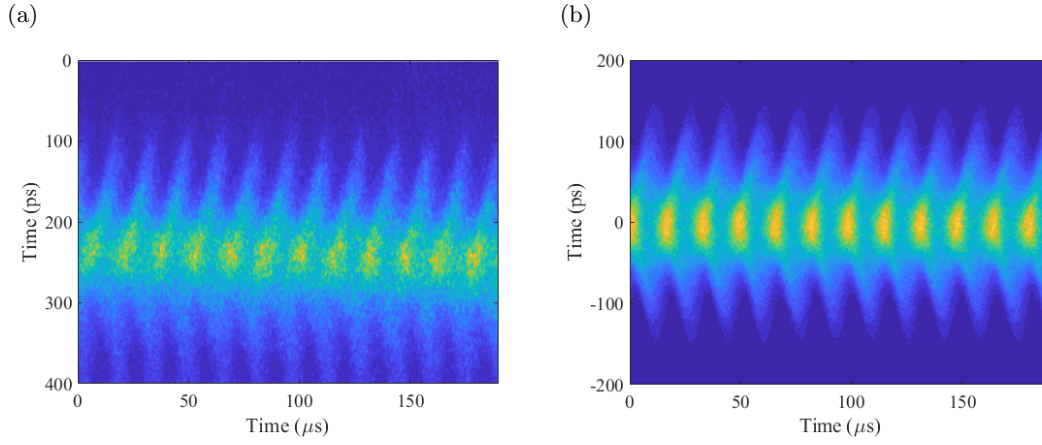


FIG. 11. The experimental result (left, Fig.11(a)) of the longitudinal electron distribution observed by the visible light streak camera. The upper side of the vertical axis corresponds to the head of the bunch. The modulation frequency is settled as the maximum bunch length condition. The right figure (Fig.11(b)) is the simulation result whose modulation frequency is settled as the maximum bunch length condition on Fig.6.

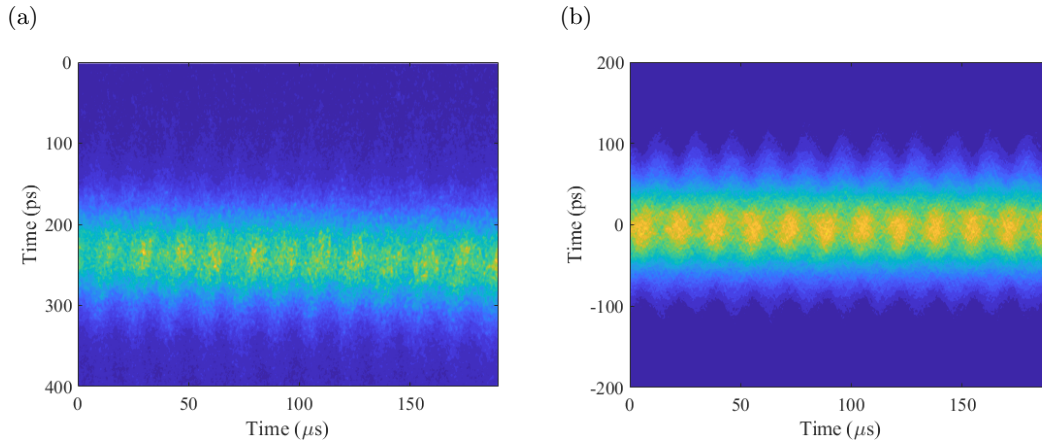


FIG. 12. The experimental result (left, Fig.12(a)) of the longitudinal electron distribution observed by the visible light streak camera. The modulation frequency is settled as -1 kHz from the maximum bunch length condition. The right figure (Fig.12(b)) is the simulation result whose modulation frequency is settled as -1 kHz from the maximum bunch length condition on Fig.6.

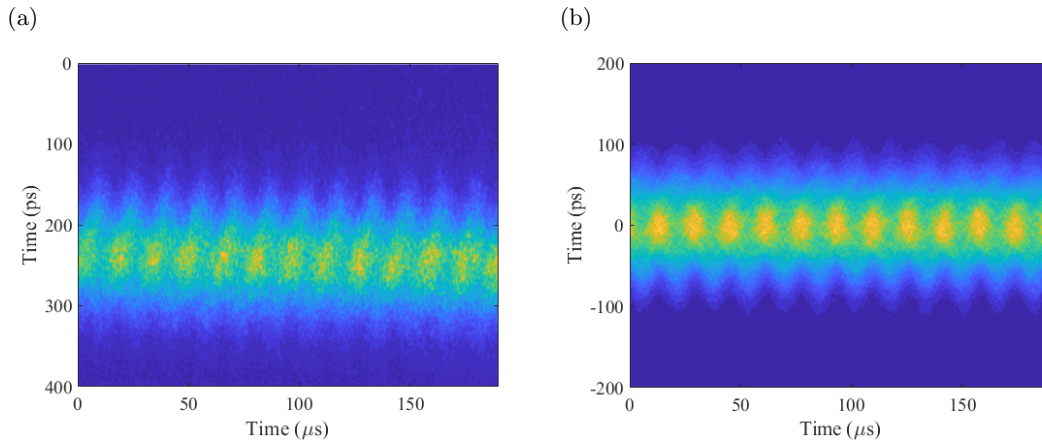


FIG. 13. The experimental result (left, Fig.13(a)) of the longitudinal electron distribution observed by the visible light streak camera. The modulation frequency is settled as +1 kHz from the maximum bunch length condition. The right figure (Fig.13(b)) is the simulation result whose modulation frequency is settled as +1 kHz from the maximum bunch length condition on Fig.6.

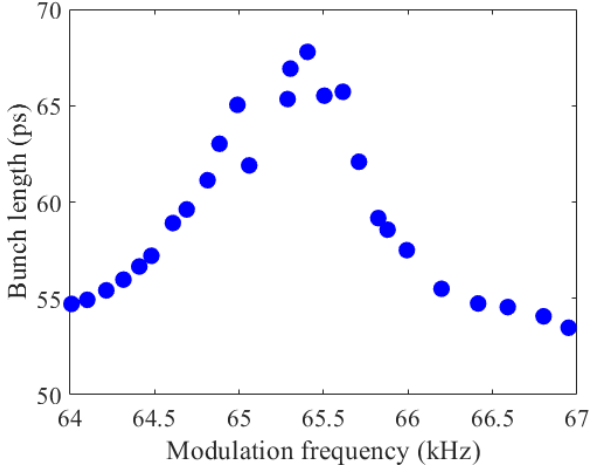


FIG. 14. The experimental result of the detuning curve for the bunch lengthening under the phase modulation. The set value of the modulation amplitude was 3 degree (52.4 mrad). The horizontal axis corresponds to the modulation frequency which is near to the twice of the synchrotron frequency.

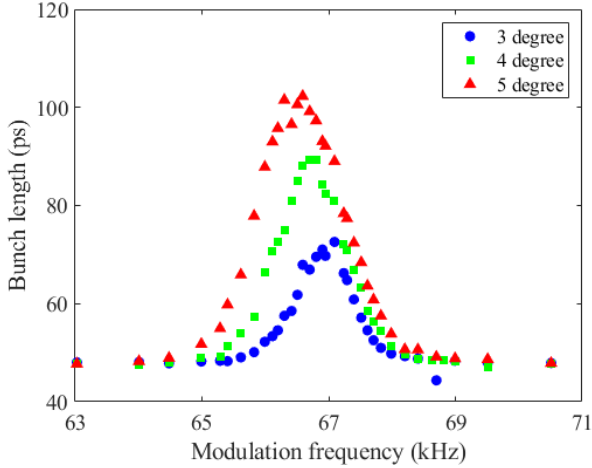


FIG. 15. The experimental result of the detuning curve for the bunch lengthening under the phase modulation with different 3 set values of the modulation amplitudes; 3 degree (blue circles), 4 degrees (green squares), and 5 degrees (red triangles).

the simulation. The detuning curve from the experiment showed an asymmetric shape around the peak frequency, which was near twice the synchrotron frequency. This tendency of the asymmetry agreed with the theoretical conclusion and the simulation results. According to the simulation, the detuning curve has a negative detuning property for twice the synchrotron oscillation frequency. However, this negative detuning was not clear because of the uncertainty of the measurement of the synchrotron oscillation frequency. According to the simulation result in Fig.6, the negative detuning frequency expected in this case is 600 Hz. To identify this slight detuning

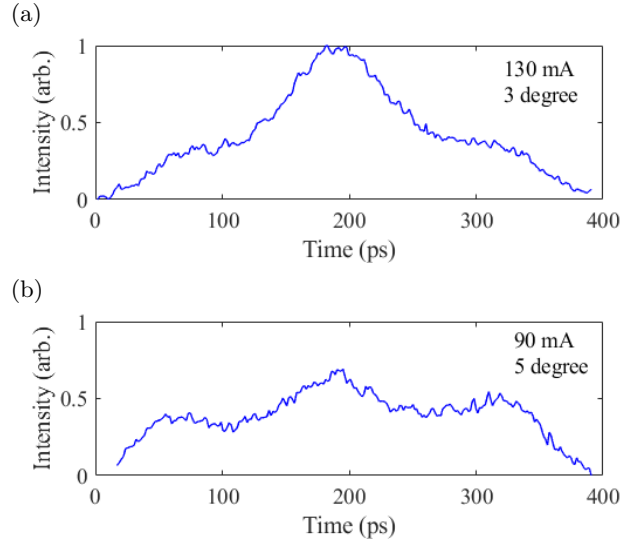


FIG. 16. The longitudinal profile of the electron beam with the modulation amplitude of 3 degrees (upper, Fig. 16(a) and 5 degree (lower, Fig. 16(b) at the peak frequencies for each detuning condition. The beam current conditions for each data were 130 mA (Fig. 16(a)) and 90 mA (Fig. 16(b)). The vertical scales for both figures are normalized one to show the figures properly.

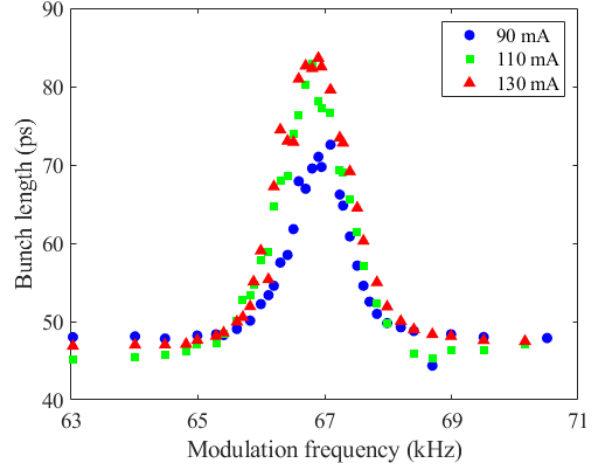


FIG. 17. The experimental result of the detuning curve for the bunch lengthening under the phase modulation with different 3 beam current conditions; 90 mA (blue circles), 110 mA (green squares), and 130 mA (red triangles).

frequency clearly, we have to measure the synchrotron frequency with better precision than 300 Hz, which is not the precision we can realise easily. To improve the precision of the measurement could be one issue to understand the beam dynamics in-depth. In the experiment, we could confirm that the bunch lengthening due to the phase modulation becomes prominent under the more extensive amplitude condition. In such condition, the negative detuning property becomes prominent with

larger modulation amplitude due to the non-linearity of the electron beam motion. The bunch lengthening becomes larger under higher beam current condition due to the transient beam loading effect, which is shown in the simulation results, too.

As already discussed in the preceding studies[11–16], the phase modulation scheme can improve the beam quality by improving the beam lifetime and stabilise the coupled bunch instabilities. In parallel, however, the energy spread can oscillate under the phase modulation. This

change in the energy spread could lead to a degradation of the synchrotron radiation beam, especially for the beam from the undulators and other insertion devices. Therefore, it is essential to optimise the parameters of the phase modulation, the modulation amplitude and frequency, to improve the beam stability by keeping the quality of the synchrotron radiation beam. To search for these optimum conditions which work both on the electron beam and the synchrotron radiation beam, now we consider the next steps in collaboration with the beamlines in KARA storage ring.

-
- [1] P. Bramham, S. Hansen, A. Hofmann, and E. Peschardt, Longitudinal instabilities of bunched beams in the ISR (1977), CERN-ISR-RF-TH/77-20.
- [2] H. Frischholz, S. Hansen, A. Hofmann, and E. P. nand W. Schnell, Longitudinal stabilization of bunched beams in the ISR by a higher harmonic cavity (1977), CERN-ISR-RF-TH/77-41.
- [3] A. Hofmann and S. Myers, Beam dynamics in a double RF system (1980), CERN-ISR-RF-TH/80-26.
- [4] Y. Miyahara, S. Asaoka, G. Isoyama, A. Mikuni, H. Nishimura, K. Soda, and H. Kanzaki, Landau damping of the longitudinal coupled-bunch instability on an electron storage ring, *Jpn. J. Appl. Phys.* **22**, L733 (1983).
- [5] J. M. Byrd, S. D. Santis, M. Georgsson, G. Stover, J. D. Fox, and D. Teytelman, Commissioning of a higher harmonic rf system for the advanced light source, *Nucl. Instrum. Methods A* **455**, 271 (2000).
- [6] G. Skripka, Å. Andersson, A. Mitrovic, P. F. Tavares, F. J. Cullinan, and R. Nagaoka, Commissioning of the harmonic cavities in the MAX IV 3 GeV ring, in *Proceedings of 7th International Particle Accelerator Conference* (2016) p. 2911.
- [7] Y. Chae and J. Keil, Control of collective effects by active harmonic cavity in an MBA-based light source with application to the PETRA upgrade, in *Proceedings of 9th International Particle Accelerator Conference* (2018) p. 1433.
- [8] B. Bravo, J. M. Alvarez, A. Salom, and F. Perez, HOM damped normal conducting 1.5 GeV cavity design evolution for the 3rd harmonic system of ALBA storage ring, in *Proceedings of 10th International Particle Accelerator Conference* (2019) p. 2498.
- [9] M. P. Kelly, Z. A. Conway, M. Kedzie, S. MacDonald, T. Reid, G. P. Zinkann, and U. Wienands, Superconducting harmonic cavity for bunch lengthening in the APS upgrade, in *Proceedings of 19th International Conference on RF Superconductivity* (2019) p. 717.
- [10] H. Feng, S. D. Santis, K. Baptiste, W. Huang, C. Tang, and D. Li, Proposed design and optimization of a higher harmonic cavity for ALS-U, *Rev. Sci. Instrum.* **91**, 014712 (2020).
- [11] S. Sakanaka, M. Izawa, T. Mitsunashi, and T. Takahashi, Improvement in the beam lifetime by means of an rf phase modulation at the KEK Photon Factory storage ring, *Phys. Rev. ST-AB* **3**, 050701 (2000).
- [12] S. Sakanaka and T. Obina, Observation of longitudinal quadrupole-mode oscillation of a bunch which were introduced by RF phase modulation in the electron storage ring, *Jpn. J. Appl. Phys.* **40**, 2465 (2001).
- [13] N. P. Abreu, R. H. A. Farias, and P. F. Tavares, Longitudinal dynamics with rf phase modulation in the Brazilian electron storage ring, *Phys. Rev. ST-AB* **9**, 124401 (2006).
- [14] M. Sommer, M. Höner, B. Isbarn, S. Khan, B. Riemann, and T. Weis, Coupled-bunch instability suppression using rf phase modulation at the delta storage ring, in *Proceedings of 6th International Particle Accelerator Conference* (2015) p. 179.
- [15] M. Sommer, B. Isbarn, B. Riemann, and T. Weis, Interaction of rf phase modulation and coupled-bunch instabilities at the delta storage ring, in *Proceedings of 7th International Particle Accelerator Conference* (2016) p. 1720.
- [16] M. Sommer, B. Isbarn, S. Kötter, B. Riemann, and T. Weis, Numerical multiparticle tracking studies on coupled-bunch instabilities in the presence of rf phase modulation, in *Proceedings of 9th International Particle Accelerator Conference* (2018) p. 3511.
- [17] <https://www.ibpt.kit.edu/kara>.
- [18] M. Toda, *Theory of oscillation (Shindou-Ron)*, New physics series (Shin-Butsurigaku Series) 3 (Baifuu-Kan, 1968).
- [19] Dimtel, inc., <https://www.dimtel.com/>.
- [20] D. Teytelman, Phase modulation in storage-ring RF system, physics.acc-ph, arXiv:1907.01381v2 (2019).
- [21] B. Kehrer, A. Borysenko, E. Hertle, N. Hiller, M. Holtz, A.-S. Müller, P. Schönfeldt, and P. Schütze, Visible light diagnostics at the anka storage ring, in *Proceedings of 6th International Particle Accelerator Conference* (2015) p. 866.
- [22] A. W. Chao, *Physics of collective beam instabilities in high energy accelerators*, Wiley series in beam physics and accelerator technology (Wiley-Interscience Publication, 1993) p. 279.
- [23] E. Blomley, M. Schedler, and A.-S. Müller, Beam studies with the new longitudinal feedback system at the anka storage ring, in *Proceedings of 7th International Particle Accelerator Conference* (2016) p. 2658.